International Journal of Technology 14(4) 749-760 (2023)
Received November 2022 / Revised January 2023 / Accepted February 2023

International Journal of Technology

http://ijtech.eng.ui.ac.id

Surface Coating Effect on Corrosion Resistance of Titanium Alloy Bone Implants by Anodizing Method

Eva Oktavia Ningrum[1*], Ianatul Khoiroh[2], Hanifah Inas Nastiti[1], Ryan Anindya Affan[1], Achmad Dwitama Karisma[1], Elly Agustiani[1], Agus Surono[1], Heri Suroto[3], S. Suprapto[1], Lulu Sekar Taji[1], Sinung Widiyanto[4]

[1]*Department of Industrial Chemical Engineering, Faculty of Vocational Studies, Institut Teknologi Sepuluh Nopember, Kampus ITS Sukolilo, Surabaya 60111, Indonesia*
[2]*Department of Chemical & Environmental Engineering, Faculty of Science and Engineering, University of Nottingham Malaysia, Jalan Broga 43500 Semenyih, Selangor, Malaysia*
[3]*Orthopedic and Traumatology Department, Faculty of Medicine, Airlangga University/Dr. Soetomo General Academic Hospital, Jl. Mayjen Prof. Dr. Moestopo No.47, Surabaya, Jawa Timur 60132, Indonesia*
[4]*Magister of Ocean Engineering, Faculty of Engineering and Marine Sciences, Hang Tuah University, Jl. Arief Rahman Hakim No.150, Keputih, Kec. Sukolilo, Surabaya 60111, Indonesia*

Abstract. In the presented work, the formation of anodic oxide film on Ti-6Al-4V ELI (Extra Low Interstitial) alloy in 0.02 M trisodium phosphate (Na_3PO_4) electrolyte solution using various voltages were investigated. The color produced by the anodizing, the intensity of TiO2 content, the thickness of the oxide layer, and the corrosion rate were examined. It was obtained that the color appearance of Ti-6Al-4V ELI could be changed easily by altering the applied voltages. The higher the voltage applied in the anodizing process, the thicker the titanium oxide layer formed. The corrosion resistance analysis in a Simulated Body Fluid revealed that the non-anodized specimen showed a higher corrosion rate compared to the anodized specimen. The increase of oxide layer thickness leads to a significant decrease in corrosion rate and consequently increases the corrosion resistance. In addition, the anodized sample achieved the highest corrosion resistance at 15 V.

Keywords: Anodizing; Corrosion resistance; Titanium oxide; Ti-6Al-4V alloy

1. Introduction

A bone implant is a medical device used to strengthen the existing bone structure or supports an injured bone structure. In this case, approximately 90% of implants in Indonesia imports. Therefore, given the rising demand for implants, the development of bone implants is a crucial debate issue. Based on the biomedical viewpoint, implant stability and the osseointegration process, which has the potential for rehabilitation, are the most important internal factors in the implantation of medical devices. Therefore, it is essential to create bone implants that have high-quality and effective when placed within the body (Dewi *et al.*, 2020; Genisa *et al.*, 2020; Izmin *et al.*, 2020). Orthopedic implants are now made from various materials, including polymers, ceramics, metals, and composites. The majority of metals are bio tolerant, although titanium and its alloys have a bioinert nature

*Corresponding author's email: eva-oktavia@chem-eng.its.ac.id, Tel.: 031-5937968; Fax.: 031-5965183
doi: 10.14716/ijtech.v14i4.6146

under specific circumstances (Koju, Niraula and Fotovvati, 2022).

Titanium Ti-6Al-4V ELI is a commonly used implant material in the medical field due to its mechanical and corrosion resistance properties (Szymczyk-Ziółkowska *et al.*, 2022; Jaafar *et al.*, 2020; Atmani *et al.*, 2018; Karambakhsh *et al.*, 2011). This corrosion resistance property emerges due to the formation of a natural oxide layer, which mainly contains TiO_2 on the titanium surface when it contacts the air (Lestari *et al.*, 2020). In addition, the Ti-6Al-4V ELI alloy material is the most commonly used material for implants in orthopedics (Kashyap, Rashid, and Khanna, 2022; Swain *et al.*, 2021; Szymczyk-Ziółkowska *et al.*, 2021; Gabor *et al.*, 2020; Kiel-Jamrozik *et al.*, 2015). Furthermore, to its advantages, this material has several weaknesses, including the thin natural oxide layer on titanium causing implant wornness, low bone bonding capacity, and incapability to prevent metal ions exposure due to implant degradation. Besides, titanium alloys also have poor osseointegration in long-term implantation (Lestari *et al.*, 2020).

Implant surface modification is necessary to obtain good implant properties and performance for the body. This surface modification is important to increase surface energy by providing surface roughness and chemical composition. This will increase tissue adhesion and implant integration as well as reduce bacterial reactions and inflammatory responses in the body (Rani and Jatolia, 2018). In this case, one of the methods that can be employed to improve implant performance is an anodizing method. Anodizing method is metal oxidation carried out in certain electrolytes by producing an electric field at the metal/electrolyte interface (Izmir and Ercan, 2019). This method is the easiest method to modify the thickness, composition, and morphology of the metal oxide layer. Moreover, the anodization process is used to restrict the infiltration process (Kiel-Jamrozik *et al.*, 2015). A thin oxide layer grows on the implant's surface during this process. Properties of the layer depend on the electrolyte, production method, oxidation time, and electric parameters of the process (Kiel-Jamrozik *et al.*, 2015; Szewczenko *et al.*, 2015; Ziębowicz, Ziębowicz and Bączkowski, 2015; Al-Mobarak and Al-Swayih, 2014; Indira, Mudali and Rajendran, 2013; Fadl-allah, Quahtany and El-Shenawy, 2013; Bhola *et al.*, 2011; Szewczenko *et al.*, 2010; Narayanan and Seshadri, 2007; Nagy *et al.*, 2005; Van-Gils *et al.*, 2004; Roessler *et al.*, 2002).

According to prior research, some inorganic ions, such as molybdate and metavanadate, can passivate titanium in solutions of sulfuric and hydrochloric acids (Mogoda, Ahmad, and Badawy, 2004). Anodizing has also been performed in phosphoric acid solutions under different conditions to improve the corrosion resistance of Ti−6Al−4V alloy in the simulated physiological environment such as (Karambakhsh, Afshar, and Malekinejad, 2012) conducted anodizing on the Ti-6Al-4V alloy in phosphoric acid electrolyte and evaluated its corrosion resistance in 3 different solutions (Ringer's solution, artificial saliva solution, and a mixture of Ringer's solution + H_2O_2). The research further resulted that the higher the voltages, the higher the corrosion resistance obtained due to the passivity produced by the anodizing process. Furthermore, Martinez, Flamini, and Saidman (2022) studied the impact of inhibitor anions on the alloy corroded in Ringer solution. In this case, galvanostatic anodization of Ti–6Al–4V alloy with inorganic inhibitors such as Na_2MoO_4, NaH_2PO_4, and NH_4VO_3 solutions produced colorful thin oxide layers. Their findings demonstrated that, regardless of the solution employed, compact, amorphous oxides free of pores or fractures may be produced. The alloy anodized in Na_2MoO_4 solution had the lowest corrosion current density. In addition, no signs of corrosion or fractures were seen (Martinez, Flamini and Saidman, 2022).

(Tamilselvi, Raman and Rajendran, 2006) also evaluated the corrosion of Ti-6Al-4V ELI alloy using the electrochemical impedance spectroscopy method in a Simulated Body Fluid (SBF) solution. This solution was used to simulate the physiological conditions in the body.

In addition, to develop the color chart of the Ti-6Al-4V alloy, anodizing was also carried out in trisodium phosphate electrolyte (Wadhwani *et al.*, 2018).

Research concerning the anodizing process of Ti-6Al-4V alloy has been numerously conducted; however, it is only limited to the use of corrosion resistance test solution, causing its inability to simulate the body's physiological condition. Therefore, the current research used SBF solution. The effect of various voltage on the implant color visual, the mass of the oxide layer formed, oxide film thickness, and implant corrosion resistance were investigated in this study. Moreover, the correlation between film thickness and its corrosion resistance was also elucidated. In addition, the trisodium phosphate electrolyte solution was chosen because it provides better corrosion resistance compared to the acidic electrolyte solution (Karambakhsh *et al.*, 2015).

2. Materials and Methods

2.1. Materials

The main material used in this research was Ti-6Al-4V ELI metals act as an anode that would be layered by TiO_2 using an anodizing method. An aluminum foil sheet was also used as a cathode. The electrolyte used was 2 g of trisodium phosphate dodecahydrate purchased from Merck, which initially dissolved in 1000 mL aquadest. Titanium wire 28 AWG 0.3 mm and alligator clip were also employed as the supporter of both Ti-6Al-4V ELI metal and aluminum foil during the anodizing process. The electrical power source was obtained from DC Power Supply WANPTEK of NPS 1203W 120V/3A type. In addition, a SBF solution was used as an electrolyte during the potentiodynamic polarization analysis to investigate the corrosion rate of anodized Ti-6Al-4V ELI metal material.

2.2. Methods

Anodizing method was done in Na_3PO_4 (base solution) electrolyte solution. In this case, the Ti-6Al-4V specimen obtained pre-treatment to make the implant surface shiny so that the anodizing color produced can be seen clearly. This pre-treatment process used Ti-6Al-4V ELI metals, previously polished using *langsol* or green stone to obtain a mirror-like surface. The solution used for anodizing was Trisodium Phosphate solution with a concentration of 0.02 M of 250 mL volume. The cathode was aluminum foil, and the anode was the Ti-6Al-4V specimens. Anodizing process was performed within 30 s for each sample, the variable parameter being the anodizing voltage. Anodizing was performed in the 15-75 V voltage range, and with the steps of 15 V. The schematic apparatus for an anodizing process is shown in Figure 1.

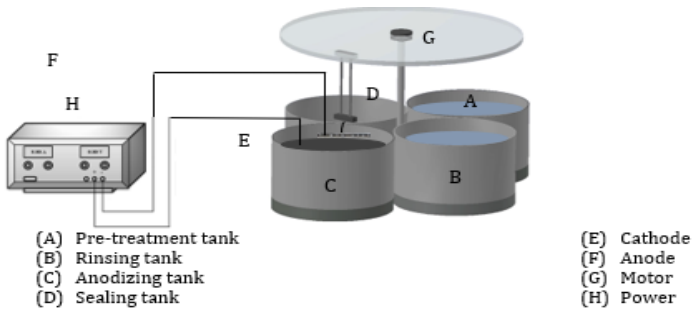

Figure 1 Anodizing experiment setup

2.2.1. XRD Analysis

XRD was used to identify the titanium oxide crystal component formed after anodizing.

2.2.2. Spectrophotometry Analysis

Spectrophotometry Analysis was carried out to determine the quantitative parameters of the specimen surface color (Konica Minolta CM-5 spectrophotometer). In order to measure the color difference of each specimen, this tool would obtain data values of L*, a*, and b*, where chromaticity was obtained using the CIELAB color space method based by using Equation (1)

$$\text{Chromaticity} = \sqrt{a^2 + b^2} \quad (1)$$

The wavelength formed from each color can be obtained through the visible light spectrum. The refractive index value was calculated using Equation (2) to determine the thickness of the oxide layer formed.

$$n_o = 5{,}193 + \frac{2.441 \times 107}{\lambda^2 max - 0.803 \times 107};\ t = \frac{\lambda max}{4 n_o} \quad (2)$$

Where,

t = Oxide layer thickness (nm)

λ = Maximum wavelength (nm)

n_o = Refractive index film

2.2.3. Potentiodynamic Polarization Analysis

This analysis was done to investigate the corrosion behavior of the titanium specimen without and after anodizing. Potentiodynamic polarization involved the CorrTest tool equipped with CS Studio 5 software. This tool series consists of three electrodes; those are: the referral electrode (SCE, *Saturated Calomel Electrode*), the working electrode (titanium specimen), and the assistant electrode (Graphite). In addition, an SBF solution at a pH of 7.4 was employed to investigate the titanium corrosion behavior (Tamilselvi, Raman and Rajendran, 2006). In this case, the pH of human blood was in the range of 7.35-7.45 (Bakr *et al.*, 2021). The following table further lists the composition of the SBF solution.

Table 1 SBF Solution Composition

No	Reagent	Composition (g/L)
1.	NaCl	8.00
2.	KCl	0.40
3.	$CaCl_2$	0.18
4.	$NaHCO_3$	0.35
5.	$Na_2HPO_4.2H_2O$	0.48
6.	$MgCl_2.6H_2O$	0.10
7.	KH_2PO_4	0.06
8.	$MgSO_4.7H_2O$	0.10
9.	**Glucose**	**1.00**

3. Results

3.1. Analysis of Anodizing Results in Trisodium Phosphate Electrolyte

3.1.1. Effect of Voltage on the Implant Color Visual

During the anodizing process, each voltage results in a different color. This interference color is caused by stoichiometric defects in oxide layer composition or wave interference on the crystal layer (Kahar *et al.*, 2020). Based on the anodizing process, it was obtained that goldish brown, dark blue, light blue, yellow, and goldish yellow colors were produced from a voltage of 15, 30, 45, 60, and 75 V, respectively, shown in Figure 2.

Figure 2 Anodized Ti-6Al-4V at 15, 30, 45, 60, and 75 Volts (from left to right)

3.1.2. Effect of Voltage on the Mass of Oxide Layer Formed

Based on Faraday's Law I, the mass formed on the anode after the anodizing process can be obtained using Equation (3)

$$W = \frac{e\,i\,t}{96500} \quad (3)$$

As data comparison, in addition to using a theoretical equation, data collection was also conducted by weighing the titanium specimen mass, both before and after the anodizing process, to investigate the mass of the oxide layer formed after the anodizing process. Figure 3 indicates the addition of mass in each anodizing voltage variety based on Faraday's Law I equation. In this case, there was an increase in titanium oxide mass from 15 V voltage to 75 V voltage. Such results are in accordance with the previous literature that the higher the voltage for the anodizing process, the thicker the titanium oxide layer formed (Wadhwani *et al.*, 2018). This is in line with Δmass obtained from the experimental method using an analytical scale that mass addition resulting from 15 V to 75 V voltage shows an increasing trend. Hence, based on the comparison between these data, the higher voltage given during anodizing process, the thicker the oxide layer formed on the titanium specimen.

Based on the theoretical calculation conducted, the Δmass addition anomaly occurred at 45 V to 60 V, indicating the most significant increase compared to the other voltages. In this case, the Δmass increase occurred was more than 100% from 45 to 60 V. This occurred due to the current formed during the anodizing process. Furthermore, it was known that from 45 V to 60 V the increased current was quite high from 0.090 A to 0.48 A. This current increase occurred due to the instability of electrode distance during the anodizing process, where the closer the distance of the electrode, the higher the current (Alphanoda, 2016). Furthermore, Figure 3 shows the difference in mass formed (ΔMass) obtained from both theoretical and experimental calculations.

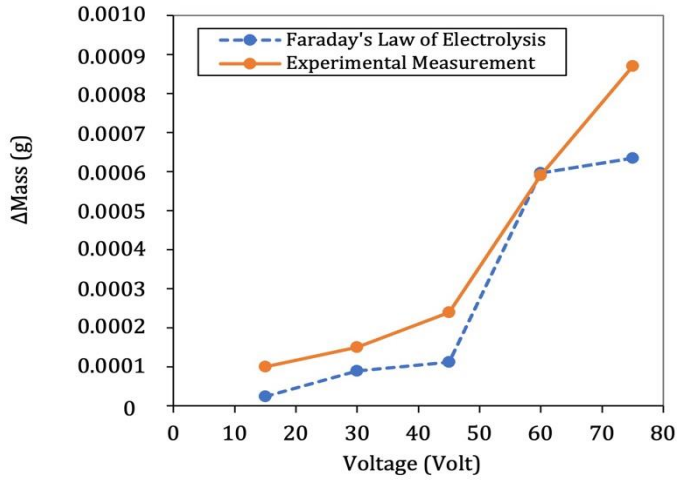

Figure 3 Effect of Voltage on TiO_2 Mass Formed

3.2. Analysis of XRD

The peak of 2θ angle measurement indicates the presence of TiO_2 (Titanium Oxide) based on ICDD standards, which are at 35°, 38°, 40°, 53°, 58°, 64°, 67°, 71°, 75°, 77°, 78°, 82°, and 88° (*International Centre for Diffraction Data,* 2022). Figure 4 further shows that the three titanium specimens resulting from the anodizing results (15, 45, and 75 Volt) have different intensities of titanium oxide content at a certain peak. This difference indicates that the peak of 53° and 71° at 75 V provided the highest TiO_2 intensity percentage compared to 15 and 45 V. This test also further showed that the highest anodizing results in terms of TiO_2 among the voltage of 15, 45, and 75 V was obtained at 75 V. Based on this difference, the higher the voltage provided in anodizing process, the more oxide content produced (added oxide layer thickness) (Izmir and Ercan, 2019; Napoli *et al.*, 2018). Based on this explanation, anodizing at a voltage of above 75 V produce higher TiO_2 intensity as well.

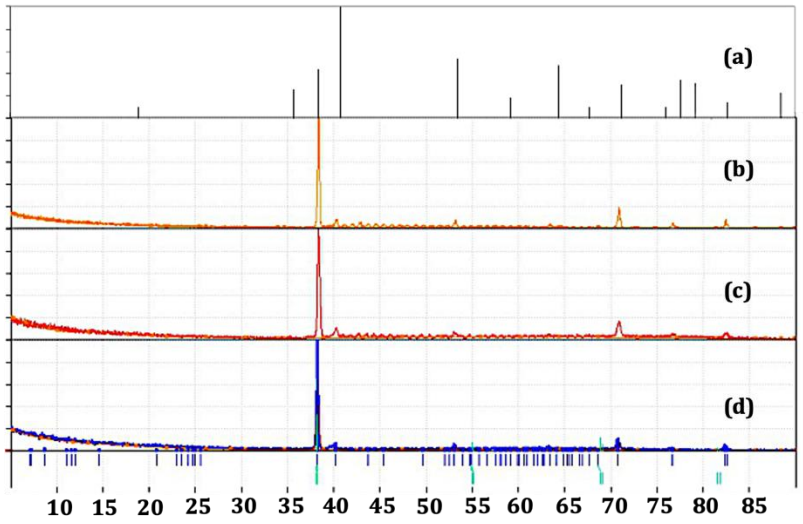

Figure 4 XRD Analysis spectrum of Ti-6Al-4V specimen (a) Titanium Oxide Reference of ICDD Standard No. 98-009-9784 and XRD Analysis spectrum after Anodizing Process at (b) 75 Volt, (c) 45 Volt, (d) 15 Volt

3.3. Analysis of Spectrophotometry Results

This analysis aimed to measure the color parameter and difference in each specimen. Thus, qualitative and quantitative data can be obtained. This method was carried out using a *spectrophotometer* tool, where the color score can be obtained using CIELAB (*standard colorimetric space)* (Napoli *et al.*, 2018). Based on the test that has been done, the color parameter data obtained were L*, a*, dan b*. Furthermore, based on the value of L*, a*, dan b*, the chromatic score can be determined by substituting the a and b values into Equation (1).

Table 2 L*, a*, b* Parameter and Chromaticity

No	Variable	L*	a*	b*	*Chromaticity*
1.	15 Volt	46.75	-0.47	-0.44	0.207
2.	30 Volt	49.25	-0.36	-7.51	28.264
3.	45 Volt	49.61	-1.03	-3.83	7.864
4.	60 Volt	50.67	-1.67	-2.04	3.475
5.	75 Volt	64.47	5.40	9.65	61.141

Table 2 above shows that the highest lightness was obtained at a voltage of 75 Volt, which produced goldish yellow. This lightness parameter would be further used to know the brightness level of the color. Meanwhile, a high chromatic score was obtained at a

voltage of 30 V by 28.264 and at 75 V by 61.141. In this case, chromaticity is defined as the quality of light characterized by a dominant wavelength. Based on this description, L*, a*, and b* parameters on CIELAB *color space* were used to investigate color quality produced by the anodizing process, which has no correlation with the oxide layer thickness produced.

3.3.1. Effect of Voltage on Oxide Film Thickness

The thickness of the oxide layer was determined using the calculation of the interference colors method approach. This method can measure the thickness of the oxide layer by determining the light spectrum wavelength with the resulting anodizing color. Furthermore, the wavelength was determined using a *visible spectrum chart.* After the wavelength was obtained, the *refractive index* value was also obtained. This *refractive index* value would further determine the thickness of the oxide layer. In this case, the thickness of the titanium oxide layer and *refractive index* from the wavelength value was obtained using Equation (2), as presented in Table 3. Based on Table 3 indicates that the higher the voltage, the longer the wavelength obtained. The Refractive index was inversely proportional to the thickness of the oxide layer. The lower the refractive index value, the greater the oxide layer thickness

Table 3 Film Thickness of Titanium Oxide (TiO_2)

No	Voltage	Wavelength (nm)	*Refractive index* (n_0)	Thickness of Oxide Layer (nm)
1.	15 V	380	1.448	65.596
2.	30 V	469	1.438	81.543
3.	45 V	535	1.429	93.626
4.	60 V	583	1.421	102.580
5.	75 V	608	1.416	107.307

Table 3 shows that the oxide layer thickness is directly related to anodizing voltage. As shown above, the thickness of the oxide layer increased by increasing voltage from 15-75 V. In this case, the highest oxide layer was obtained at 75 V by 107.307 nm, while the lowest was at 15 V by 65.596 nm. This is in accordance with the report by (Karambakhsh *et al.*, 2011) that the addition of voltage in the anodizing process produces an increase in the oxide layer, which leads to an increase in mass produced. This difference further provides different *interference color visuals* as well, according to the voltage variety. The increase in TiO_2 film thickness was caused by the greater the applied voltage, so the greater the current delivered. This causes more TiO_2 to be deposited at the Ti-6Al-4V anode.

3.4. Effect of Voltage on Implant Corrosion Resistance

Table 4 shows I_{corr} (A/cm^2, E_{corr} (Volt) value and *corrosion rate*, indicating the potentiodynamic test results in each specimen, both before and after anodizing process. Table 4 shows that the non-anodized titanium specimen had the highest corrosion rate compared to the anodized titanium specimen by 0.092707 mmpy. In addition, the lowest corrosion rate was reached at 15 V by 0.0033486 mmpy. Based on the potentiodynamic test, a significant corrosion rate decrease occurred between non-anodized and anodized specimens at 15 V by 96%. This occurred due to the oxide layer thickness effect. The oxide layer on the non-anodized specimen was only 2-5 nm. However, the anodized specimen at 15 V obtained an oxide layer of 65.596 nm. The increase of oxide layer thickness by 92% (60.595 nm) caused a significant decrease in corrosion rate. Corrosion resistance increases (corrosion rate decreases) as the increase of layer thickness (Saraswati *et al.*, 2020).

Table 4 Corrosion Resistance of non-anodized and anodized specimens

No	Variable	E_{corr} (Volts)	I_{corr} (Amps/cm^2)	Corrosion Rate (mmpy)
1	Non-anodized	-1.31E-01	1.21E-06	9.27E-02
2	15 V	1.97E-03	4.38E-08	3.35E-03
3	30 V	-1.76E-02	4.46E-08	3.42E-03
4	45 V	-6.61E-02	1.04E-07	7.94E-03
5	60 V	1.83E-01	1.13E-07	8.68E-03
6	75 V	1.87E-01	1.25E-07	9.56E-03

Based on the potentiodynamic analysis obtained, the Tafel curve is shown in Figure 5. From this Tafel curve, it can be seen the effect of Ecorr and Icorr on the corrosion rate. The higher the I corr, the higher the corrosion rate. It was also found that the higher the voltage or the current, the greater the corrosion rate, according to Equation 4.

$$CR = K1 \times Icorr/\rho \times EW \quad (4)$$

where

CR = corrosion rate (mm/yr) for icorr (μA/cm^2)
K1 = 0.1288 (mpy.g/A.cm^2)
Icorr = exchange current density
ρ = density (g/cm^3)
EW = equivalent weight

The corrosion rate is directly proportional to its Icorr. Even though anodizing may reduce the corrosion rate when compared to without anodizing, there still be a percentage increase in corrosion rate as the anodizing voltage increases.

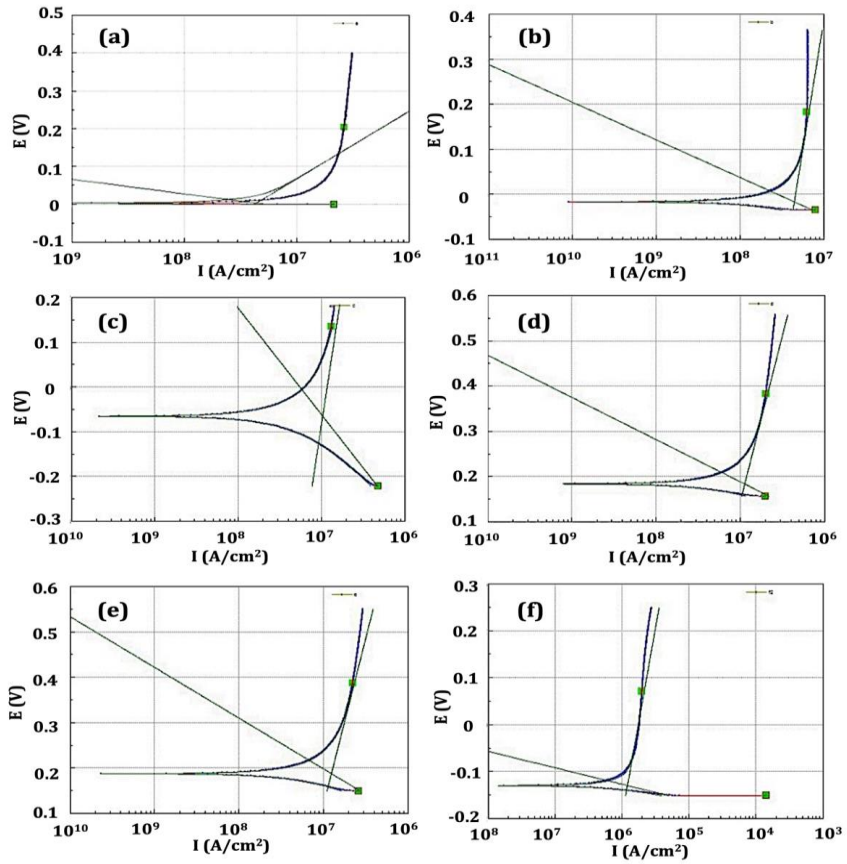

Figure 5 Tafel Curve in Each Voltage Variety (a) 15V, (b) 30V, (c) 45V, (d) 60V, (e) 75V, and (f) non-anodized specimen

Table 5 shows that the effect of voltage on corrosion rate was not quite significant, where there was an increased corrosion rate by 2% at 15 V to 30 V, 9% at 45 V to 60 V, and 10% 60 V to 75 V. This indicates that voltage in a fixed anodizing time variable was not quite significant in affecting the corrosion rate, where the corrosion rate tends to be constant at 15-30 V and at 45-75 V. However, an anomaly occurred in the corrosion rate increase from 30V to 45V by 57%. Based on the testing on the anodized titanium specimen, there was an insignificant increase in corrosion rate in each voltage variable. This occurred because TiO_2 layer thickness had not yet been complete during the anodizing process at 45-75 V in 30 seconds because the higher the voltage, the higher the current given. When the current provided during the anodizing process is higher, the time spent on the anodizing process also increases. In this case, the anodizing process is considered complete when the current value (*A-COARSE*) on the *power supply* shows a decrease approaching zero. In addition, this increase can also cause higher porosity than the surface layer as the voltage increases, hence increasing the corrosion rate (Karambakhsh *et al.*, 2011).

Table 5 Layer Thickness and Corrosion Rate for anodized and non-anodized Ti-6Al-4V specimen

No	Variable	Thickness of Layer (nm)	Δt	CR (mmpy)	ΔCR
1	Non-anodized	2 – 5	-	9.27E-02	-
2	15 V	65.596	60.596	3.35E-03	8.94E-02
3	30 V	81.543	15.947	3.42E-03	6.80E-05
4	45 V	93.626	12.083	7.94E-03	4.52E-03
5	60 V	102.580	8.954	8.68E-03	7.36E-04
6	75 V	107.307	4.727	9.56E-03	8.81E-04

4. Conclusions

The anodizing process using Na_3PO_4 electrolyte solution produces different colors in various voltages by the interference color phenomenon. Based on spectrophotometry analysis revealed that a high chromatic score was obtained at a voltage of 75 V. From the refractive index indicates that the higher the voltage, the longer the wavelength obtained. Higher voltage in the anodizing process produces an increase in the oxide layer, which leads to an increase in mass produced. Moreover, based on the potentiodynamic analysis obtained that increasing the voltage or the current result in a higher corrosion rate. The XRD analysis indicates the presence of TiO_2 based on the ICDD standard in all voltages employed. Increasing the anodizing voltage increased the oxide film thickness, consequently increasing the TiO_2 content in the specimen. Furthermore, the corrosion resistance analysis in a Simulated Body Fluid revealed the non-anodized specimen showed a higher corrosion rate compared to the anodized specimen. The increase of oxide layer thickness leads to a significant decrease in corrosion rate and consequently increases the corrosion resistance. Therefore, in future work, the anodized implant of Ti-6Al-4V ELI in this work will be further evaluated by comparing it with other electrolytes such as hydroxide, organic acid, sulfuric acid, and friendly inorganic salt electrolytes in various concentrations.

Acknowledgments

The current study was supported by a Research Grant of "Penelitian Produk Vokasi Unggulan Perguruan Tinggi 2022" from The Ministry of Education, Culture, Research, and Technology (KEMENDIKBUDRISTEK TAHUN 2022 (1919/PKS/ITS/2022).

References

Al-Mobarak, N.A., Al-Swayih, A.A., 2014. Development of Titanium Surgery Implants for Improving Osseointegration Through Formation of a Titanium Nanotube Layer. *International Journal of Electrochemical Science*, Volume 9(1), pp. 32–45

Alphanoda, A.F., 2016. Effect of Anode-Cathode Distance and Coating Duration on Corrosion Rate on Hard Chrome Electroplating Results (Pengaruh Jarak Anoda-Katoda dan Durasi Pelapisan Terhadap Laju Korosi pada Hasil Electroplating Hard Chrome). *Jurnal Teknologi Rekayasa*, Volume 1(1), pp. 1–6

Atmani, D., Saoula, Nadia., Abdi, A., Azzaz, M., Wang, Y., Mohamedi, M., 2018. Structural, Morphological, and Electrochemical Corrosion Properties of TiO_2 Formed on Ti6Al4V Alloysby Anodization. *Crystal Research and Technology*, Volume 53(12), pp. 1–7

Bakr, M., Thabet, H., Ghandour, N., Farrag, A,, Mohamed, R.E., 2021. Histological and Ultrastructural Changes of White Blood Cells in Vitro Storage of Human Blood at Different Time Intervals. *Egyptian Journal of Histology*, Volume 45(3), pp. 849–862

Bhola, R*.,* Bhola, M., Mishra, B., Ayers, R.A., Olson, D.L., Ohno, T., 2011. Surface Characterization of Anodically Treated β - Titanium Alloy for Biomedical Applications. *Электронная Обработка Материалов*, Volume 47(4), pp. 75–82

Dewi, A.H., Yulianto, D.K., Ana, I.D., Rochmadi, Siswomihardjo, W., 2020. Effect of Cinnamaldehyde, an Anti-Inflammatory Agent, on the Surface Characteristics of a Plaster of Paris – $CaCO_3$ Hydrogel for Bone Substitution in Biomedicine. *International Journal of Technology,* Volume 11(5), pp. 963–973

Fadl-allah, S.A., Quahtany, M., El-Shenawy, N.S., 2013. Surface Modification of Titanium Plate with Anodic Oxidation and Its Application in Bone Growth. *Journal of Biomaterials and Nanobiotechnology*. Volume 4(1), pp. 74–83

Gabor, R., Doubkove, M., Gorosova, S., Malanik, K., Vandrovcoca, M., Cvrcek, L., Drobikova, K., Kutlakova, K.M., Bacakova, L., 2020. Preparation of Highly Wettable Coatings on Ti–6Al–4V ELI Alloy for Traumatological Implants Using Micro-Arc Oxidation in An Alkaline Electrolyte. *Scientific Reports*, Volume 10(1), pp. 1–16

Genisa, M., Shuib, S., Ahmad Rajion, Z.A., Mohamad, D., Arief, M.E., 2020. Dental Implant Monitoring Using Resonance Frequency Analysis (RFA) and Cone Beam Computed Tomography (CBCT) Measurement*. International Journal of Technology,* Volume 11(5), pp. 1015–1024

Indira, K., Mudali, K.U., Rajendran, N., 2013. Corrosion Behavior of Electrochemically Assembled Nanoporous Titania for Biomedical Applications. *Ceramics International*. Volume 39(2), pp. 959–967

Izmin, N.A.N., Hazwani, F., Abdullah, A.H., Todo, M., 2020. Risk of Bone Fracture in Resurfacing Hip Arthroplasty at Varus and Valgus Implant Placements. *International Journal of Technology*. Volume 11(5), pp. 1025-1035

Izmir, M., Ercan, B., 2019. Anodization of Titanium Alloys for Orthopedic Applications. *Frontiers of Chemical Science and Engineering,* Volume 13(1), pp. 28–45

Jaafar, A., Hecker, C., Árki, P., Joseph, Y*.,* 2020. Sol-Gel Derived Hydroxyapatite Coatings for Titanium Implants: A Review. *Bioengineering*, Volume 7(4), p. 127

Kahar, S., Singh, A., Patel, V., Kanetkar, U., 2020. Anodizing of Ti and Ti Alloys for Different Applications: A Review. *International Journal for Scientific Research & Development*, Volume 8(5), pp. 272–276

Karambakhsh, A., Afshar, A., Ghahramani, S., Malekinejad, P*.,* 2011. Pure Commercial Titanium Color Anodizing and Corrosion Resistance. *Journal of Materials Engineering and Performance*, Volume 20(9), pp. 1690–1696

Karambakhsh, A., Afshar, A., Malekinejad, P., 2012. Corrosion Resistance and Color

Properties of Anodized Ti-6Al-4V. *Journal of Materials Engineering and Performance*, Volume 21(1), pp. 121–127

Karambakhsh, A., Ghahramani, S., Afshar, A., Malekinejad, P., 2015. Comparison of the Corrosion Resistance of Alkaline- and Acid Anodized Titanium. *Materials Performance*, Volume 54(1), pp. 51–55

Kashyap, N., Rashid, R.A., Khanna, N., 2022. Carbon Emissions, Techno-Economic and Machinability Assessments to Achieve Sustainability in Drilling Ti6Al4V ELI for Medical Industry Applications. *Sustainable Materials and Technologies*, Volume 33, pp. 175–194

Kiel-Jamrozik, M., Szewczenko, J., Basiagi, M., Nowińska, K., 2015. Technological Capabilities of Surface Layers Formation on Implant Made of Ti-6Al-4V ELI Alloy. *Acta of Bioengineering and Biomechanics*, Volume 17(1), pp. 31–37

Koju, N., Niraula, S., Fotovvati, B., 2022. Additively Manufactured Porous Ti6Al4V for Bone Implants: A Review, *Metals*, 12(4), p. 687

Lestari, F.P., Sari, Y.R., Rokhmanto, F., Asmaria, T., Pramono, A.W., 2020. Surface Modification of Ti-6Al-4V Alloy By Anodization Technique at Low Potential to Produce Oxide Layer. *Journal of Electronics*, Volume 2(3), pp. 93–102

Martinez, A.L., Flamini, D.O., Saidman, S.B., 2022. Corrosion Resistance Improvement of Ti-6Al-4V Alloy by Anodization In The Presence of Inhibitor Ions. *Transactions of Nonferrous Metals Society of China*, Volume 32(6), pp. 1896–1909

Mogoda, A.S., Ahmad, Y.H., Badawy, W.A., 2004. Corrosion Inhibition of Ti-6Al-4V Alloy in Sulfuric and Hydrochloric Acid Solutions Using Inorganic Passivators. *Materials and Corrosion*, Volume 55(6), pp. 449–456

Nagy, P.M., Ferencz, B., Kálmán, B., Djuričić, B., Sonnleitner, R., 2005. Morphological Evolution of Ti Surfaces During Oxidation Treatment. *Materials and Manufacturing Processes*, Volume 20(1), pp. 105–114

Napoli, G., Paura, M., Vela, T., Schino, A.D., 2018. Colouring Titanium Alloys By Anodic Oxidation. *Metalurgija,* Volume 57(1–2), pp. 111–113

Narayanan, R., Seshadri, S.K., 2007. Phosphoric Acid Anodization of Ti-6Al-4V - Structural and Corrosion Aspects. *Corrosion Science*, Volume 49(2), pp. 542–558

Rani, S., Jatolia, S.N., 2018. Electrodeposited Hap Coatings on Titanium Alloys: A Review. *International Journal of Research and Analytical Reviews,* Volume 847(4), pp. 847–853

Roessler, S., Zimmermann, R., Scharnweber, D., Werner, D., Worch, H., 2002. Characterization of Oxide Layers on Ti6Al4V and Titanium by Streaming Potential and Streaming Current Measurements. *Colloids and Surfaces B: Biointerfaces*, Volume 26(4), pp. 387–395

Saraswati, W.C., Anawati, A., Jujur, I.N., Gumelar, M.D., 2020. Effect of Coloring by Anodizing on the Corrosion Behavior of Ti-6Al-4V Alloy. *In*: AIP Conference Proceedings, Volume 2232(1). pp. 1–5

Swain, S., Misra, R.D.K., You, C.K., Rautray, T.R., 2021. TiO_2 Nanotubes Synthesised on Ti-6Al-4VELI Exhibits Enhanced Osteogenic Activity: A potential Next-Generation Material to Be Used as Medical Implants. *Materials Technology*, Volume 36(7), pp. 393–399

Szewczenko, J., Basiaga, M., Kiel-Jamrozik, M., Kaczmarek, M., Grygiel, M., 2015. Corrosion Resistance of Ti_6Al_7Nb Alloy After Various Surface Modifications. *Solid State Phenomena*, Volume 227, pp. 483–486

Szewczenko, J., Walke, W., Nowinska, K., Marciniak, J., 2010. Corrosion Resistance of Ti-6Al-4V Alloy After Diverse Surface Treatments. *Materialwissenschaft und Werkstofftechnik*, Volume 41(5), pp. 360–371

Szymczyk-Ziółkowska, P., Hoppe, V., Gąsiorek, J., Rusińska, M., Kęszycki, D., Szczepański, Ł.,

Dudek-Wicher, R., Detyna, J., 2021. Corrosion Resistance Characteristics of a Ti-6Al-4V ELI Alloy Fabricated by Electron Beam Melting After the Applied Post-Process Treatment Methods. *Biocybernetics and Biomedical Engineering*, Volume 41(4), pp. 1575–1588

Szymczyk-Ziółkowska, P., Ziółkowski, G., Hoppe, V., Rusińska, M., Kobiela, K., Madeja, M.,Dziedzic, R., Junka, A., Detyna, J., 2022. Improved Quality and Functional Properties of Ti 6Al-4V ELI Alloy for Personalized Orthopedic Implants Fabrication with EBM Process. *Journal of Manufacturing Processes*, Volume 76(1), pp. 175–194

Tamilselvi, S., Raman, V., Rajendran, N., 2006. Corrosion Behaviour of Ti-6Al-7Nb and Ti-6Al-4V ELI Alloys in the Simulated Body Fluid Solution by Electrochemical Impedance Spectroscopy. *Electrochimica Acta*, Volume 52(3), pp. 839–846

Van-Gils, S., Mast, P., Stijins, E., Terryn, H., 2004. Colour Properties of Barrier Anodic Oxide Films on Aluminium and Titanium Studied with Total Reflectance and Spectroscopic Ellipsometry. *Surface and Coatings Technology*, Volume 185(2–3), pp. 303–310

Wadhwani, C., Brindis, M., Kattadiyil, M., O'Brien, R., Chung, K.H., 2018. Colorizing Titanium 6Aluminum-4Vanadium Alloy Using Electrochemical Anodization: Developing a Color Chart. *Journal of Prosthetic Dentistry*, Volume 119(1), pp. 26–28

Ziębowicz, A., Ziębowicz, B., Bączkowski, B., 2015. Electrochemical Behavior of Materials Used in Dental Implantological Systems. *Solid State Phenomena*, Volume 227, pp. 447–450